Synthesis and Characterization of Zn doped Li(Li$_{0.21}$Mn$_{0.54}$Ni$_{0.125}$Co$_{0.125}$)O$_2$ as the Layer Materials For Battery Applications

S.Rumh. Kadhim[2], R. Etefagh[1,2,4,*] and H. Arabi[2,3]

[1]Department of Physics University Campus University of Guilan, Rasht, Iran
[2]Renewable energies, Magnetism and nanotechnology research laboratory, Departments of Physics, Faculty of Science, Ferdowsi University of Mashhad, Mashhad, Iran
[3]Research center for Hydrogen Storage and Litium- Ion Battery, Faculty of Science, Ferdowsi University of Mashhad, Mashhad, Iran
[4]Department of Physics, Payame Noor University, P. O. BOX 19395-3697, Tehran, Iran

Abstract: *In this paper, pure and impure nanopowders of Li(Li$_{0.021}$Mn$_{0.54}$Ni$_{0.125}$Co$_{0.125}$)O$_2$ were prepared with different percentages) x= (%0.10 ,%0.075 ,%0.05 ,%0.02of Zn impurity by sol-gel method, and the effect of different percentages were investigated on the structural, physical and chemical properties of the samples. These properties of samples characterized by X-ray diffraction (XRD), field-scattering microscopy (FESEM), X-ray energy spectroscopy (EDS), transmission electron microscopy (TEM), thermogravimetric analysis (TGA), differential thermal analysis (DTA), infrared spectroscopy (FTIR), and the results of characterization were investigation. All the reflection peaks indicate that the samples have standard α-NaFeO$_2$ layered structure with the space group R3m, except for the super lattice ordering between 22°-25°.The FESEM images have shown that these nanoparticles have Hexagonal structures for doped and undoped nanopowders. The particle size of nanopowders in the range of 30-80 nm the chemical analysis of EDS has proven the presence of Zn in the samples. TG /DTA measurements showed weight loss in pure and impure of nanopowders. In infrared spectroscopy (FTIR), the connection bonds and chemical elements used in these nanopowders have been investigated.*

1. INTRODUCTION

Today, the lithium ion battery as a justly new member in the battery technology has been widely studied due to its promising applications in the field of laptops, cell phones, digital cameras and hybrid electric vehicles [1-3].Other cathode materials such as spinel LiMn$_2$O$_4$ [4] and olivine LiFePO$_4$ [5] have been successfully applied in lithium ion batteries, but they typically have very low capacities and also usually do not perform very well. Among all the cathode materials of LIBs the novel Li-rich Mn-based layered solid-solution system adjusted as Li$_2$MnO$_3$.LiMO$_2$(M=Co, Ni and Mn) has recently become the focus of researches because of its higher capacities(over 250 mAh/g good rate performance and improved safety comparing to conventional LiCoO$_2$ cathode materials[6]. Although this kind of cathode material has many attracting advantages, it has a poor rate performance and is subject to voltage

decay after long cycling.

Over the past few years, many effective methods have been performed to enhance the electrochemical performance of layered lithium cobalt nickel manganese oxide material, such as new synthesis methods bulk doping [7,8], surface coating [9] and composite material designing.

Doping one or more metal elements have been demonstrated to be one effective method to promoting the cycling stability and has been widely used in modification of cathode materials and has also successfully been used for improving Li-rich layered materials [10, 11, and 12].The transition element in the oxide materials can be substituted by metal elements such as Zn [13], Zr [14], Mo [15], Mg [16] and those doped materials show higher cyclic performance and structural stability surface modification, i.e. coating, is also one useful method for improving one cathode material. In recent years, many researchers have employed this method for improving Li-rich layered material [17, 18, 19, 20, 21].

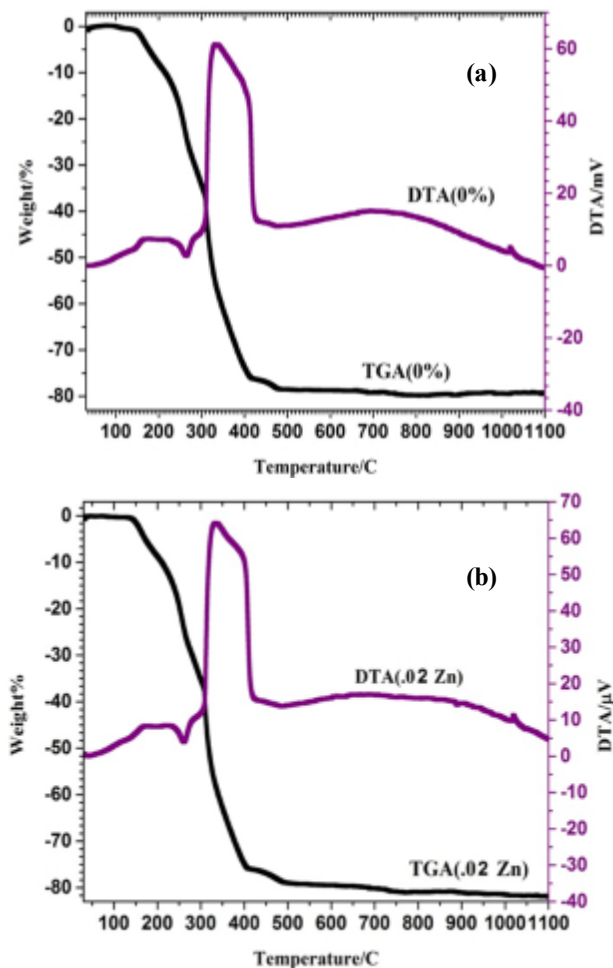*To whom correspondence should be addressed: Email: Bahar_3036@yahoo.com

Figure 2. XRD patterns of $(Li_{0.21}Mn_{0.54}Ni_{0.125}Co_{0.125-x})Zn_xO_2$ nanopowders with different Zn content (0.02%, 0.05%, 0.075%, 0.10%).

Figure 1. a) TG/DTA curves of the pure dry gel of $Li(Li_{0.21}Mn_{0.54}Ni_{0.125}Co_{0.125})O_2$, b) TG/DTA curves of the Zn doped $Li(Li_{0.21}Mn_{0.54}Ni_{0.125}Co_{0.125-x}) Zn_xO_2$

In the group of Li-rich layered cathode materials, $Li[Li_{0.2}Mn_{0.54}Ni_{0.13}Co_{0.13}]O_2$ have been widely investigated already and always shows better performance [19, 22-28]. because of that the presence of cobalt reduces the electrode polarization significantly and improves the activation of the Li_2MnO_3 component[22], but it still contains 13 mol% of Co which certainly represents an issue with regard to cost, and the effect of the cobalt seems to deteriorate the high-potential cycling performances of the materials[29, 30].

The sol–gel method has many advantages; for instance, it can achieve the molecular-level mixing of the raw materials and precursors, it requires relatively low temperature treatment, small and narrow diameter distribution of products can be produced, simple equipment and easy operation are needed and so on [31].

In this work $Li(Li_{0.21}Mn_{0.54}Ni_{0.125}Co_{0.125-x})Zn_xO_2$ was prepared by a sol–gel method using the citric acid as the chelating agents and different percent Zn. The effects of the doping on the structural and chemical performance of these nanoparticles were investigation.
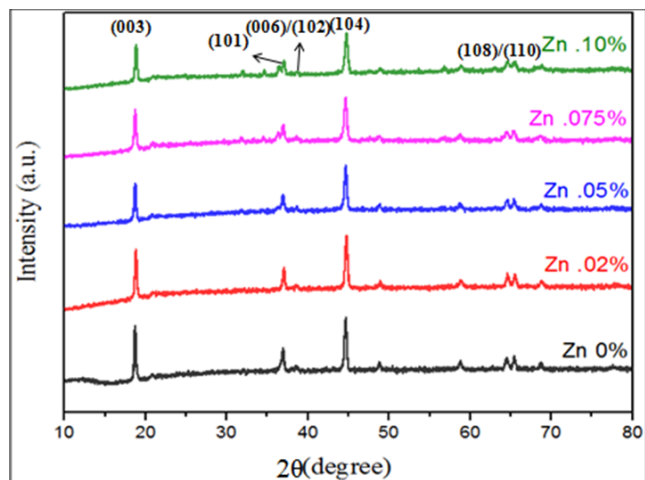
2. EXPERIMENTAL DETAILS

1.2. Preparation of materials

$Li(Li_{0.21}Mn_{0.54}Ni_{0.125}Co_{0.125-x})Zn_xO_2$ nanopowders were prepared with the precursors of pristine and Zn-doped samples from pure materials of $CoN_2O_6.4H_2O$, $NiN_2O_6.6H_2O$, $C_4H_6MnO_4.4H_2O$, $Li(NO_3)$ and $Zn(NO_3)_3 \cdot 4H_2O$ by sol-gel method in which citric acid was used as a chelating agent as the synthesis method. Firstly mixture was dissolved in to aqueous solutions, and then citric acid was dropped slowly into aqueous solution under stirring at 80°C until gel-like was obtained. The molar ratio of citric acid to total metal ions was unity. The gel was dried at 120°C in vacuum oven for 18h. The resulting gel precursor was decomposed at 500°C for 5 h in air to eliminate the organic substances. The decomposed powders heated at 80°0C for 6h. The final material was obtained by quenching the pellet in air to room temperature. The crystal structure of the as-prepared $Li(Li_{0.021}Mn_{0.54}Ni_{0.125}Co_{0.125-x})Zn_xO_2$ powders with different percent Zn (0.02%, 0.05%, 0.075%, 0.10%) were characterized by XRD with a D8 Advance Bruker YT diffractometer using CuKα radiation in the 2θ range of 10° and 80°. The size and morphology of the sample was investigated using FESEM performed on MIRA3TESCAN-XMU microscope equipped with a Thermo NORAN system 6 X-Ray microanalysis system supported by a NanoTrace LN-Cooled Si (Li) detector for Energy-dispersive X-ray Spectroscopy (EDS) analysis. The TEM analysis for pure and impure nanopowders was performed on an) Leo912 AB). The TG/DT analysis for pure nanopowders was performed on an STA PT1600 TG/DTA (LINSEIS) using a heating rate of 10°C/min in air. The infrared spectra were recorded using Fourier-transformed infrared spectrophotometer (AVATAR 370, Thermo Nicolet) in transmission mode in the wave number region between 4000cm^{-1} and 500 cm^{-1}.

3. RESULTS AND DISCUSSION

Figure 1(a) and 1(b) show the TG/DTA curves obtained for pure nanopowder and zinc doped $Li(Li_{0.21}Mn_{0.54}Ni_{0.125}Co_{0.125-x})Zn_xO_2$

Synthesis and Characterization of Zn doped Li(Li$_{0.21}$Mn$_{0.54}$Ni$_{0.125}$Co$_{0.125}$)O$_2$ as the Layer Materials For Battery Applications / J. New Mat. Electrochem. Systems
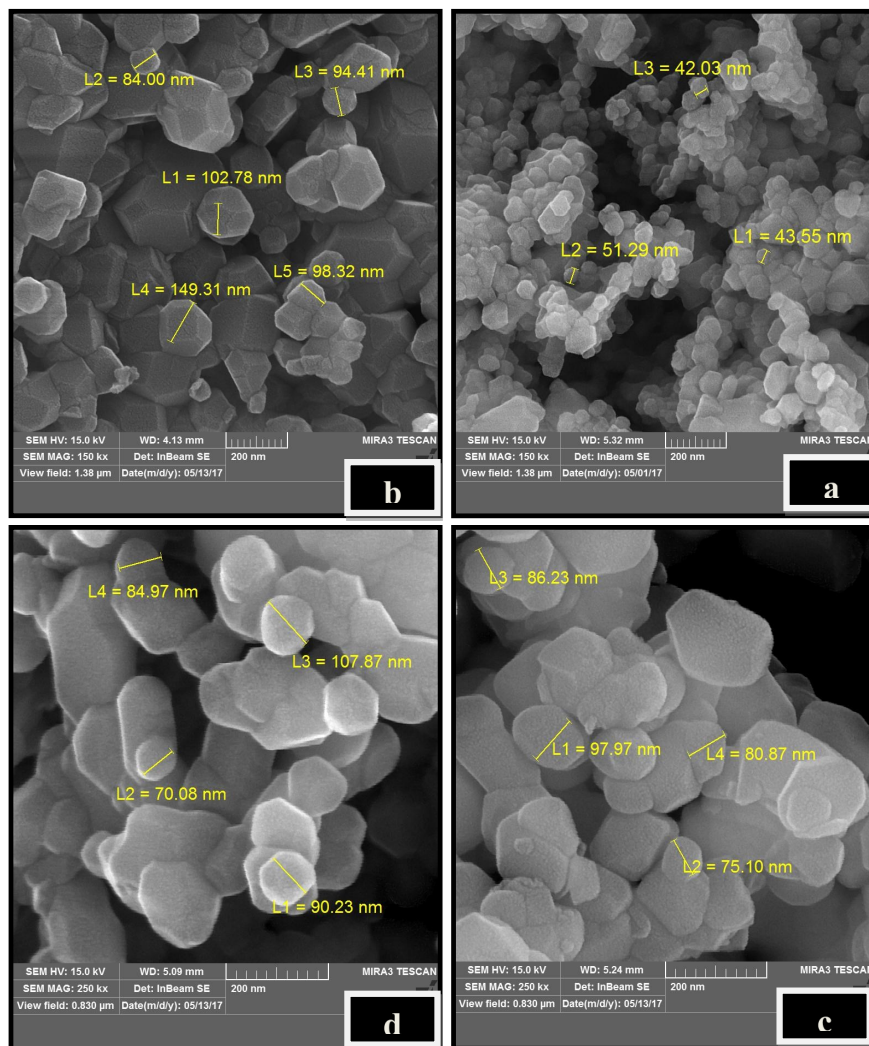
129

Figure 3. FESEM images of a) pure nanopowders, b) nanopowders with 0.02% Zn, c) nanopowders with 0.05% Zn, d) nanopowders with 0.075% Zn
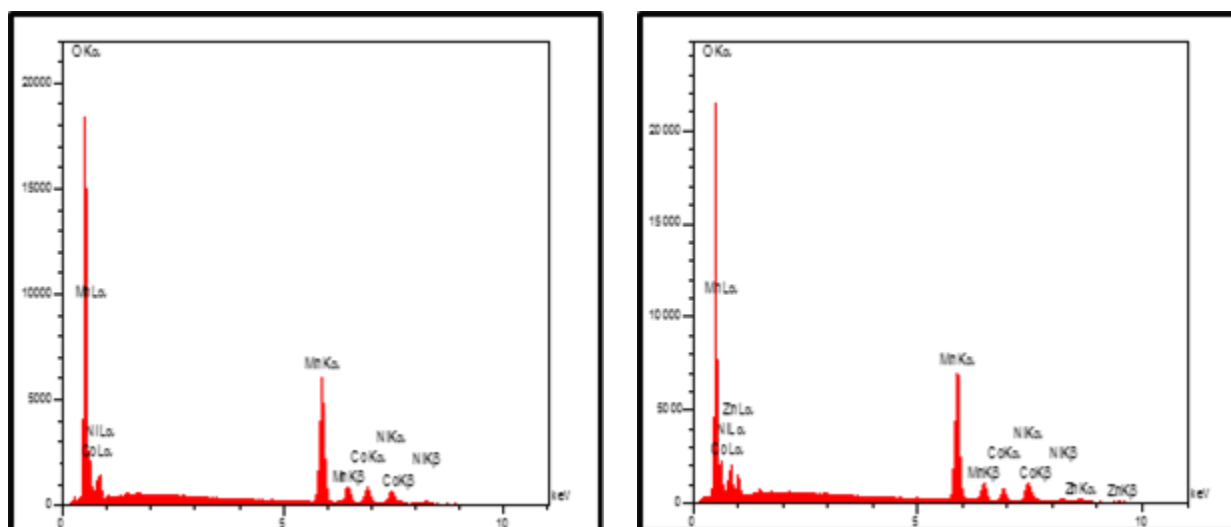
Figure 4. EDS images of Li(Li$_{0.21}$Mn$_{0.54}$Ni$_{0.125}$Co$_{0.125-x}$)Zn$_x$O$_2$ nanopowders for (a:x=0 and b:0.02%)
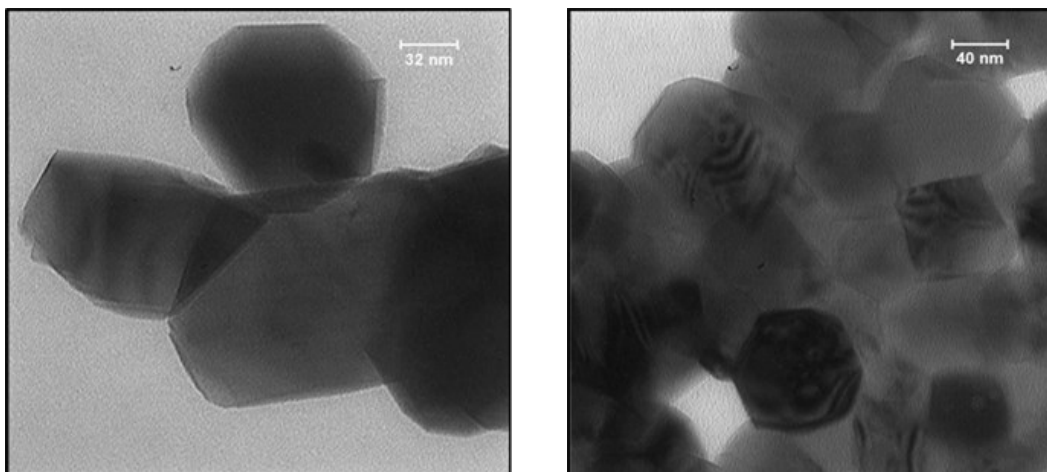
Figure 5. TEM image of Li(Li$_{0.21}$Mn$_{0.54}$Ni$_{0.125}$Co$_{0.125-x}$)Zn$_x$O$_2$ of nanopowders for x=0 and .02% Zn
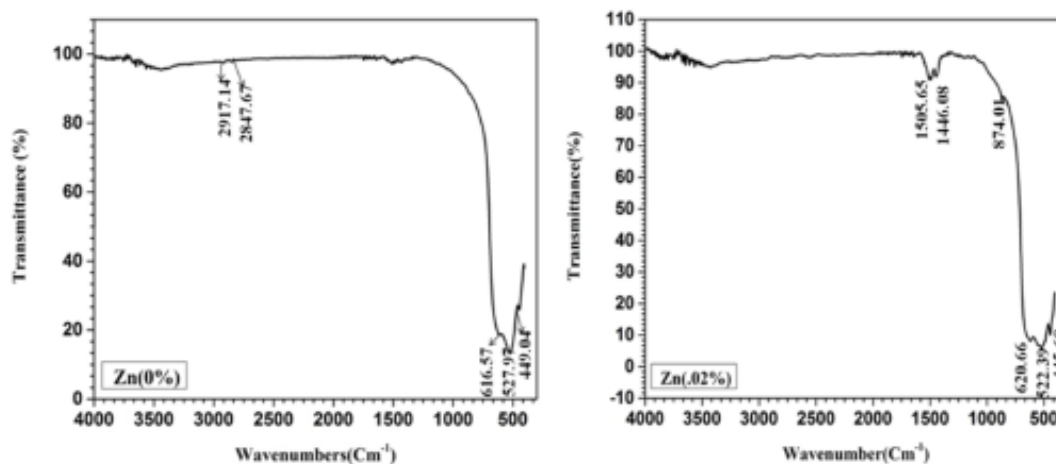
Figure 6. FTIR spectra of Li(Li$_{0.21}$Mn$_{0.54}$Ni$_{0.125}$Co$_{0.125-x}$)Zn$_x$O$_2$ nanopowders (x=0% and 0.02%)

prepared by sol gel methode. The weak endothermic peak at about 260°C in the DTA curve, which corresponds to a weight loss of 20% in the TG curve, is for the removal of residual water in the pure nanopowders gel. In the range of 300–500°C, a weight loss of 80% is indicated, which accompanies a strong exothermic Peak at 320°C. Above 500°C, there is neither any obvious weight loss nor endothermic/exothermic peak. The second weight loss is attributed to the decomposition of organic linkers in air and the residual weight percent is assigned to the remaining metal oxides. With the presence of impurity of Zn in pure crystals, these curves are almost identical [32]. Only in the DTA curve there is a peak at 900°C, possibly due to the presence of zinc melting point in this range.

The XRD patterns of the pristine and Zn doped of nanopowders are shown in Figure 2. All the reflection peaks indicate that the samples have standard α-NaFeO$_2$ layered structure with the space group R⁻3m, except that the weak peaks in the 2θ range of 20–25° identified as the (020) and (110) reflection are attributed to the monoclinic Li$_2$MnO$_3$ phase (C2/m space group)[33]. Some weak peaks of impurity phase ZnO between 30°-35° are observed in the

patterns when the amount of Zn-doping increases to 0.10%, which these peaks showed that a part of Zn cannot enter into the lattice of Li-rich structure but exist in the form of impurities due to the excess amount of Zn. the diffraction patterns show clear splitting of the hexagonal characteristic doublets of (006)/(102) and (108)/(110); and formation of cation ordered phase and indicate the good structure of layered oxides [34].

The morphologies of the layered composites before and after Zn modification are revealed in Figure 3. It is found that the Zn-doping does not change their morphologies and All the pure and impure with Zn materials have a similar morphology and it can be seen that the as-prepared homogeneous nanoparticles have a nearly spherical and hexagonal morphology with the size in the range of 40-150 nm which would simplify the intercalate and deintercalate process for Li+ and improve ion conductivity and rate performance. The EDS images of these samples (take x=0.02% as an example) are showed in Figure 4 and It can be seen that the Zn elements are distributed in the samples homogenously.

The structural, morphology and size distribution information

Synthesis and Characterization of Zn doped Li(Li$_{0.21}$Mn$_{0.54}$Ni$_{0.125}$Co$_{0.125}$)O$_2$ as the Layer Materials For Battery Applications
/ J. New Mat. Electrochem. Systems

131

about Li(Li$_{0.21}$Mn$_{0.54}$Ni$_{0.125}$Co$_{0.125-x}$)Zn$_x$O$_2$ for x=0 and .02%Zn of nanopowders were further studied by transmission electron microscopy(TEM) studies is shown in Figures 5. The TEM images of nanopowders showing that the particles have nearly hexagonal and have the average grain size 60-100nm. With additions Zn impurity the size of nanoparticles to a certain extent is greater than the pure nanopowders.

Figure 6 are shown the FTIR spectra of Li(Li$_{0.21}$Mn$_{0.54}$Ni$_{0.125}$Co$_{0.125-x}$)Zn$_x$O$_2$ nanopowders (take x=0% and 0.02% as an example) recorded in between 500 and 4000 cm^{-1}. As can be seen in figure 6, for pure nanopowders two peaks at 2917Cm^{-1} and 2847Cm^{-1}, most often indicate the residual CO$_2$ in the atmosphere, which disappears with adding Al impurity. In FTIR spectra with 0.02% Zn Two weak bands have been created in the 1507Cm^{-1} and 1429Cm^{-1}the peaks in these regions represent the asymmetric and symmetric stretching of –COO$^-$ group. Peaks below 1500Cm^{-1} confirm the presence of metal oxygen in vibration frequencies [35].

4. CONCLUSION

In this paper, Li(Li$_{0.21}$Mn$_{0.54}$Ni$_{0.125}$Co$_{0.125-x}$)Zn$_x$O$_2$ nanopowders with different percents Zn (x=0.02%, 0.05%, 0.075% and 0.10%) has been successfully synthesized by a sol–gel method using citric acid as chelating agent.XRD, FESEM, TEM, FTIR and TG/DTA were employed to study the structural, chemical and thermal properties of prepared nanopowders. The structural results for pure and impure nanopowders showed the single phase layered with the super lattice structure originating from the monoclinic Li$_2$MnO$_3$ and the as-prepared pure and impure of nanopowders have a nearly hexagonal morphology with an average diameter of approximately 40-150nm in FESEM analysis and 60-100nm for nanoparticles in TEM analysis. TG/DTA measurement for pure and impure nanopowders showed the between 300–500°C, a weight loss of 80% is attributed to the thermal decomposition of the ingredients to form Li(Li$_{0.21}$Mn$_{0.54}$Ni$_{0.125}$Co$_{0.125}$)O$_2$. FTIR spectra of Li(Li$_{0.21}$Mn$_{0.54}$Ni$_{0.125}$Co$_{0.125-x}$)Zn$_x$O$_2$ nanopowders (for x=0% and 0.02%) showed Peaks below 1500Cm^{-1} confirm the presence of metal oxygen in vibration frequencies.Finally, this study is helpful for the production of Li(Li$_{0.21}$Mn$_{0.54}$Ni$_{0.125}$Co$_{0.125-x}$)Zn$_x$O$_2$ nanopowders with different percents Zn(x=0.02%, 0.05%, 0.075% and 0.10%) as cathode material for rechargeable lithium-ion batteries.

REFERENCES

[1] Z S Peng, C R Wan, and C Y Jiang, Power Sources, 72, 215 (1998).

[2] S Bruno Electrochim. Acta, 45, 2461 (2000).

[3] E Antolini Solid State Ionics, 170, 159 (2004).

[4] Y S Lee, Y K Sun and K S Nahm Solid State Ioincs, 109, 285 (1998).

[5] Y S Hu, Y G Guo Adv. Mater., 19, 1963 (2007).

[6] D Kim, J R Croy, M M Thackeray Electrochemistry Communications, 36, 103 (2013).

[7] J. Zhao, Z.Wang, H.Guo, X.Li, Z.He, T.Li, material, Ceram. Int., 41, 9 (2015).

[8] H L Zhang, L Zhang and L Ye, Electrochem. Sci., 9, 4635 (2014).

[9] H L Zhang, L Zhang, and Sh W Yang, Electrochem. Sci., 9, 8182 (2014).

[10] P K Nayak, J Grinblat, M Levi and D Aurbach Electrochim. Acta, 137, 546 (2014).

[11] D Wang, Y Huang, Zh Q Huo and L Chen, Electrochim. Acta, 107, 461 (2013).

[12] S Yamamoto, H Noguchi and WW Zhao, Power Sources, 278, 76 (2015).

[13] H Fang, H Yi C Hu, B Yang, Y Yao, W Ma et al., Electrochimica Acta, 71, 266 (2012).

[14] K H Jeong, H W Ha, N J Yun, M Z Hong, K Kim, Electrochimica Acta, 50, 5349 (2005).

[15] J H Park, J Lim, J Yoon, K S Park, J Gim, J Song et al., Dalton transactions, 41, 3053 (2012).

[16] D. Wang Y. Huang Z. Huo L. Chen, J. Electrochimica Acta, 107, 461 (2013).

[17] S W Cho, G O Kim and K S Ryu, State Ionics, 206, 84 (2012).

[18] B Li, Q Zhang, Sh C H, Y Satob, J W Zheng, and D Ch Li, Electrochim. Acta, 59, 6748 (2011).

[19] S J Shi, J P Tu, Y Y Tang, X Y Liu, Y Q Zhang, X L Wang and et al., Electrochim. Acta, 88, 671 (2013).

[20] P K Nayak, J Grinblat, M Levi and D Aurbach, Electrochim. Acta, 137, 546 (2014).

[21] L Brian, E Kyu, T Lee and F Linda Chem. Mater., 22, 691 (2010).

[22] J Li, R Klopsch, M C Stan, S Nowak, M Kunze, M Winter et al., Power Sources, 196, 4821 (2011).

[23] J M Zheng, X B Wu and Y Yang, Electrochim. Acta, 59, 3071 (2011).

[24] X Y Liu, J L Liu, T Huang and A Sh Yu, Electrochim. Acta, 109, 52 (2013).

[25] B J Hwang, C J Wang and C H Chen, Power Sources, 146, 658 (2005).

[26] S Christopher Johnson, N Ch Li and L Christina, Chem. Mater., 20, 6095 (2008).

[27] Y Naoaki, Y Kazuhiro and M Seung Taek, J Am Chem. Soc., 133, 4404 (2011).

[28] W Jeffrey, W Fergus, Power Sources, 195, 939 (2010).

[29] L Y Yu, W H Qiu and F Lian, Mater. Letters, 62, 3010 (2008).

[30] M M Thackeray, S H Kang and C S Johnson, Electrochem. Commun., 8, 1531 (2006).

[31] A Feinle, MS Elsaesser, N Hüsing Chem Soc. Rev., 45, 12 (2016).

[32] W J Hao, H H Zhan, H Chen, Y H Wang, Q Q Tan and F B Su, Particuology, in press, 33 (2013).

[33] X Wei, P Yang, H Li, S Wang, Y Xing, X Liu and S Zhang, RSC Adv., 7 (2017).

[34] D Deivamani, P Perumal, A S Enigo Chitra and M Boomashri, Int. J. Chem. Sci., 14, 496 (2016).

[35] O Haik, N Leifer, Z Fromovich, E Zinigrad, B Markovsky, L Larush, Y Goffer, G Goobes and D Aurbach, Journal of The Electrochemical Society, 157, 10 (2010).